A Cantilevered Piezoelectric Energy Harvester Driven by Vortex-Induced Vibrations on a Cylinder in Water

Talya Feldman, Joseph Gilmartin, Evan McCauley, Brendan Merritt, and Alyssa Tepe

Professor Brian J. Savilonis

March 25th, 2022

Abstract

This Major Qualifying Project (MQP) team of seniors in Mechanical Engineering designed, built, and tested a renewable energy harvester from the flow of water through a river. This system converted the vortex-induced vibrations (VIV) of a cylinder into the bending of two cantilevers with two piezoelectric transducers attached to their fixed ends. The cantilever was designed so its natural frequency matches the vortex shedding frequency of the cylinder in a given water flow. The alternating current (AC) from the transducers was then converted into a direct current (DC) using a rectifying circuit with a diode bridge and a filter capacitor as well as a voltage regulator. This functional system, which achieved a maximum electrical power of 3.14 μW, has the capability of powering low-power electronics including temperature sensors. This can be scaled to produce more power by increasing the size of the device, particularly the piezoelectric strips, by having multiple devices of this sort beside one another to compound the output power, or by increasing the natural frequency of the resonating system.

Table of Contents

List of Figures

List of Tables

The Need

When energy comes from a source that is naturally replenished over a short time period, it is referred to as renewable energy. Renewable energy comes in many forms, which gives it flexibility in possible applications, such as solar and water (Coburn and Farhar).

Fossil fuels are thought of as a cheap and easy way to generate energy, and they are used abundantly around the world. While they might be easy, they are damaging to the environment. Switching to renewable energy and decreasing dependency on fossil fuels will reduce greenhouse emissions and harm done to the natural world. People often do not realize that renewable energy is all around. Some places to look for these energy sources are the sun, oceans, and rivers.

There are many misconceptions around renewable energy. The first misconception is that renewable energy is more expensive, but it is actually as cost effective as coal, oil, and natural gas. Another misconception is that clean energy requires too much space. In reality, space is already occupied with things such as rooftops or golf courses, where solar panels or wind farms could be added to produce clean energy (101, C., & Facts, C).

There are streams and rivers spread out throughout the United States with relative constancy. Having this almost ubiquitous source of fluid flows makes it ideal to use these rivers and streams to harvest energy. The ideal scenario would be to have a device entirely submerged in a water source that can take the flow and convert into usable energy. This project focused on making a device to harvest energy from a fluid flow with minimal disruption to the flow, which separates it from the idea of a dam to take energy from water.

In developing systems to harvest energy from currents, the Department of Energy (DOE) has some requirements set. They require these systems to have a high energy density while ensuring it does not negatively impact marine life. The DOE also looks for the device to be low maintenance and to have a long expected design life.

Background

Vortex-Induced Vibrations

When a fluid flows over a blunt object, such as a cylinder, vortices are formed behind the object. These vortices cause a change in pressure on either side of the object, leading to the object moving back and forth. As the frequency of this oscillation nears the natural frequency of the blunt object, the object can start to vibrate. (Williamson and Govardhan 414). If the mass ratio of the blunt object and the displaced fluid is decreased, the region of frequencies in which these vortex-induced vibrations (VIV) can occur becomes larger (Williamson and Govardhan 423).

VIV can have many impacts in different engineering fields. In relation to fluids, VIV can cause vibrations in heat exchanger tubes, or it can affect the dynamics of tubes that bring oil up from the ocean floor. Civil engineers need to be aware of this phenomenon when they are designing and building bridges and chimney stacks. VIV can also impact the design of vehicles, as they are made more streamlined (Williamson and Govardhan 413). VIV occurs over a large range of Reynolds numbers, and they often cause damage to engineering structures. This has led many engineers to attempt to disrupt the vortices and suppress VIV for centuries (Bernitas et al 1-2).

However, the phenomenon of VIV can be used to harvest useful renewable energy. The main parameters of VIV include Reynolds number and Strouhal number. In terms of VIV, cylinders have been well studied. The flow around a cylinder is characterized by the Reynolds number, which can be seen in Figure 1.

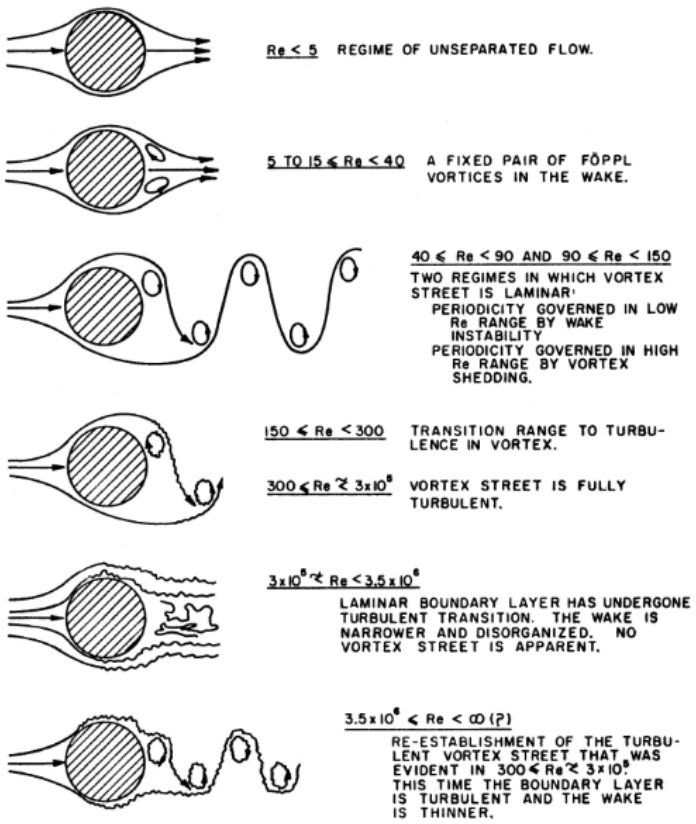

Figure 1: Various Flow Regimes Over a Cross Sectional of a Cylinder (Lienhard 3)

The Reynolds number represents the ratio of inertial forces to viscous forces and serves as an indicator of when the transition from laminar to turbulent flow occurs (Derksen 7). Reynolds number can be determined using:

$$Re = \frac{UD}{v} \tag{1}$$

Where U is the fluid's velocity over a cylinder, D is the diameter of the cylinder, and v is the kinematic viscosity of the fluid (Zahari et al. 2).

Strouhal number is another main parameter of VIV. The Strouhal number can be determined using:

$$St = \frac{f_s D}{U} \tag{2}$$

The Strouhal number (St) is related to the vortex shedding frequency (f_s) which is in hertz (Zahari et al. 2).

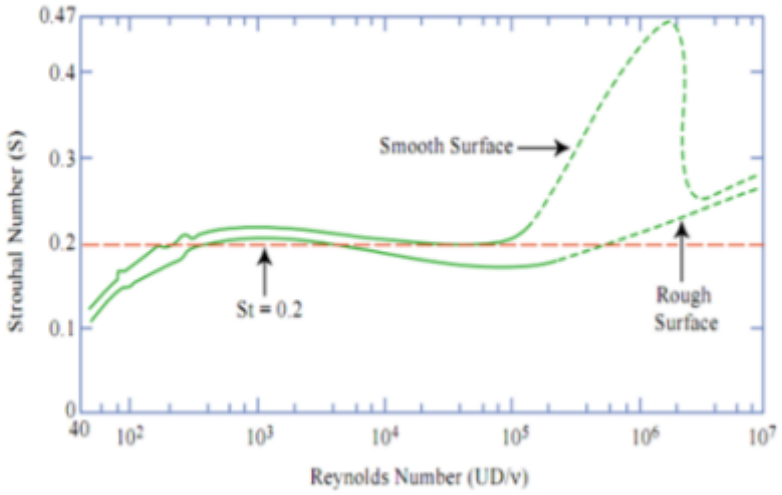

Figure 2: Strouhal Number vs. Reynolds Number (Zahari et al. 2).

The Reynolds number range of $300 < Re < 3*10^5$ is known as "Fully Turbulent Vortex Street" (Zahari et al. 2). Based on the Figure 2 above, when the Reynolds number is within the fully developed turbulent vortex street, it is commonly assumed that $St = 0.2$ (Zahari et al. 2).

A bluff body in fluid may develop a lift force. This lift force F_L can be calculated using:

$$F_L = C_L \frac{\rho U^2}{2} A \tag{3}$$

Where C_L is the time-dependent variable for lift coefficient and A is the projected area perpendicular to the fluid flow.

For a cylinder oriented perpendicularly to the fluid, A can be found using:

$$A = DL \tag{4}$$

Where D is the diameter of the cylinder and L is the length of the cylinder (*The Lift Equation*).

The maximum power in the fluid can be calculated with:

$$P_f = \frac{\rho U^3}{2} A \tag{5}$$

(Bernitas et al).

Figure 3 shows a graph plotting the Lift coefficient C_L vs the Reynolds Number Re.

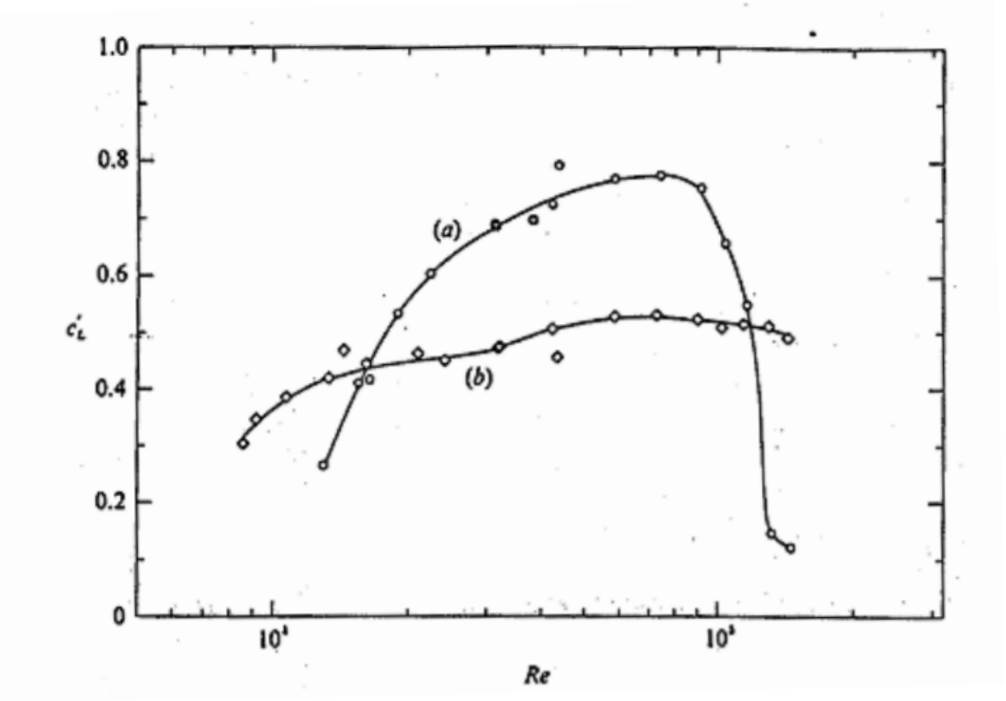

Figure 3: Lift Coefficient vs Reynolds Number Over a Cylinder

(a) $L/D = 1$, (b) $L/D = 6.7$ (Szepessy & Bearman 1992)

With the above information, frequency and force on a cylinder can give light to the amount of power that can be generated perpendicularly from fluid flow.

The VIVACE Converter

While many engineers and scientists have striven to suppress VIV, the inventors of the Vortex-Induced Vibration Aquatic Clean Energy (VIVACE) converter look instead to exploit this phenomenon. VIVACE maximizes vortex shedding to enhance the VIV and extract energy (Bernitas et al 1). This model uses cylinders immersed in a fluid flow to convert the mechanical energy into a more usable form of energy, such as electricity. These cylinders are elastically mounted in one direction, say vertically mounted. A fluid can then flow over the system horizontally, and the cylinders will move perpendicularly to both the fluid flow and their own orientation (Bernitas et al 6). VIVACE is a scalable system and can be made to extract energy from current velocities as low as 0.5 knots to 5 knots or higher. This system is also adaptable, in that it is not sensitive to environmental conditions. VIV occurs over a broad range of frequencies, as the phenomenon is not linear (Bernitas et al 1).

The diameter and length of the cylinders used for a VIVACE converter have a major impact on different aspects of the converter. The aspect ratio (L/D) of the cylinders used in the VIVACE converter is important, as this impacts the forces affecting the oscillating cylinders. The aspect ratio is recommended to be between 7 and 20 (Bernitas et al 1). Additionally, the size of the cylinders will change the mass ratio of the converter. The mass ratio, m^*, can be calculated with:

$$m^* = \frac{m_{osc}}{m_a} \tag{6}$$

Where m_{osc} is the mass of the oscillating cylinder, and m_a is the added mass of the displaced fluid.

The added mass of the displaced fluid is found using a function of the cylinder diameter and length along with the fluid density. In this sort of system, the oscillating mass includes the mass of the cylinder itself and one third of the spring mass. For higher mass ratios ($m^* >> 1$), the VIV phenomenon usually happens when the ratio (f^*) between the frequency of oscillation of the cylinder and the natural frequency (f/f_n) of the body is near one. With lower mass ratios, the body oscillates at a higher frequency and the range for VIV broadens (Bernitas et al 2).

Reduced velocity is a dimensionless parameter often used to measure vibration amplitude and is given by:

$$V_r = \frac{U}{f_n D} \tag{7}$$

Where U is the fluid velocity, f_n is the natural frequency and D is the cylinder diameter. When $m^* >> 1$ and $f^* \approx 1.0$, which means at resonance, $V_r = 1/St$. Since it can be assumed the St is 0.2, $V_r = 5$ (Williamson and Govardhan 418).

The Department of Energy (DOE) has eight different requirements that any ocean energy conversion design must satisfy to be licensed for use, and the VIVACE converter fulfills all these requirements. The first requirement is high energy density. The calculated energy from each cylinder-spring system over displaced volume of the VIVACE converter is 0.322 kW/m^3. The second requirement is that the device does not hinder navigational systems, which the VIVACE does not do, as it can remain fully submerged and extract power from currents. This converter remaining submerged also helps satisfy another requirement set by the DOE, that an ocean energy conversion device does not diminish the real estate prices in coastal areas. The converter remaining submerged means it will not be seen from shore, and therefore will not negatively impact real estate. Another concern the DOE looks to manage is whether the machine will be safe for marine life and the environment. The

oscillation of the cylinders is slow, and the vortex shedding around the machine is similar to that of fish as they swim through the water. This leads scientists to theorize minimal impact on marine life. The fifth requirement is that the device be low maintenance. In a VIVACE converter, only the cylinders are exposed. All power systems are kept within support structures and are kept such that they can be easily raised to the surface to be maintained, making the overall design low maintenance. This leads into another requirement, which is that the device be robust. As the converter is based on a nonlinear resonance, it can operate over large ranges of current velocities. The final two requirements pertain to design life and the life cycle costs. Due to the low maintenance of the design, it is expected to last twenty years, which meets the DOE's requirements. As for cost, while the initial installation has a relatively high cost, the cost of electricity converted is competitive with other converters due to the availability of the energy source and the low maintenance of the device (Bernitas et al 2, 4-5).

Vibration of a Cantilever

All objects and mechanisms will have a natural frequency based on their effective mass and effective spring constant. Cantilever systems can be modeled as spring-mass systems.

The force of a spring in static deflection can be calculated using:

$$F = kY \tag{8}$$

Where k is the spring constant and Y is the distance from the equilibrium position of the spring.

The natural frequency of a system, f_n, of a mass can be calculated using:

$$f_n = \frac{1}{2\pi}\omega_n = \frac{1}{2\pi}\sqrt{\frac{k}{m}} \tag{9}$$

Where, ω_n is the natural frequency in radians/s, and m is the mass of the object.

Because of static deflection, the spring incurs stress. In this case, the spring is a cantilevered beam. The bending normal stress, σ, at a point in a beam can be calculated using:

$$\sigma = \frac{My}{I} \tag{10}$$

Where M is the moment at the location of the beam, y is the distance from the beam's neutral axis to the point of interest, and I is the area moment of inertia of the beam. (Huston 104)

The normal bending strain of a beam, ε, can be calculated using:

$$\varepsilon = \frac{\sigma}{E} \tag{11}$$

Where E is the elastic modulus of the material (Thomson 109).

The deflection at the free end of a cantilevered beam, Y, can be calculated using:

$$Y = \frac{Fl^{3}}{3EI} \tag{12}$$

Where F is the point load at the end of the beam, l is the length of the beam, E is the elastic modulus of the material, and I is the area moment of inertia of the beam's cross sectional area (Thomson 18-37).

Therefore k from equation 8 can be derived from equation 12:

$$k = \frac{3EI}{l^{3}} \tag{13}$$

Assuming the cross sectional area is a rectangle, I can be calculated with:

$$I = \frac{WT^{3}}{12} \tag{14}$$

Where W is the width of the rectangle and T is the height of the rectangle (Huston & Josephs 15).

Taking k from equation 13, which is the effective spring constant or the stiffness, and plugging it into equation 9, the natural frequency of a beam with a mass on it can be calculated through:

$$f_{n} = \frac{1}{2\pi}\sqrt{\frac{k}{m}} = \frac{1}{2\pi}\sqrt{\frac{3EI}{ml^{3}}} \tag{15}$$

Equation 15 is used when not taking into account the effect of the mass of the beam and the effect of the displaced fluid mass. To calculate a more accurate value for the frequency of the system in water, the mass of the cantilever and displaced fluid has to be taken into account.

$$f_n = \frac{1}{2\pi}\sqrt{\frac{k}{m_{cyl}+m_a+\frac{33}{140}m_{cant}L}} \tag{16}$$

Where m_{cyl} is the mass of the cylinder, m_a is the added mass of the displaced fluid, and m_{cant} is the mass of the cantilever (Gürgöze 540; "Vibrations in Fluid–Structure").

In all systems in the real world, damping is a factor in natural frequencies. The force of damping can be calculated from:

$$F = cY' \tag{17}$$

Where *Y'* is the velocity of the spring and *c* is the damping constant, which is found experimentally for systems.

There are 3 different types of damped systems: overdamped, critically damped, and underdamped. The value of the damping ratio ζ indicates the type of system.

$$\zeta = \frac{c}{c_c} \tag{18}$$

Where c_c is the critical damping and can be calculated using:

$$c_c = 2\sqrt{km} \tag{19}$$

A system is overdamped when $\zeta > 1$, a system is critically damped when $\zeta = 1$, and a system is underdamped when $\zeta < 1$. Underdamped systems, unlike overdamped and critically damped, maintain oscillatory motion over a span of time while having a decreasing amplitude. This is the type of system that is of interest in this project. While our system will be underdamped, it is not expected to have a decreasing amplitude due to the fact that this is a forced vibration, rather than a free vibration. This is because the environment that the system will be placed in will not have the same constant energy flowing over it. By definition, that means it will be considered to have forced vibration since the water flowing from the river will never be constant and have the same energy flow through the entity.

The damped frequency f_d of an underdamped system can be calculated using:

$$f_d = f_n\sqrt{1-\zeta^2} \tag{20}$$

(Thomson 18-37).

The general equation of motion for a system under forced vibration can be written as:

$$m\ddot{Y} + c\dot{Y} + kY = F(t) \tag{21}$$

In our case, the forcing function can be assumed to be:

$$F(t) = F_L * sin(\omega t) \tag{22}$$

Where F_L is equal to the lift force (equation 3).

Thus the equation of motion for our system is:

$$m\ddot{Y} + c\dot{Y} + kY = \frac{1}{2}\rho U^2 DLC_l * sin(\omega t) \tag{23}$$

Where ω is the vortex shedding frequency in rad/s ($\omega = f_s * 2\pi$) (Blevins 61).

The response of our system can be predicted using:

$$Y(t) = Acos(\omega t - \phi) \tag{24}$$

The amplitude, A, can be calculated using:

$$A = \frac{F_L}{m\sqrt{4\omega^2(\frac{c}{2m})^2 + (\omega^2 - \omega_n^2)^2}} \tag{25}$$

When the cantilever is in resonance, the amplitude, A, can be calculated using:

$$A = \frac{F_L}{c\omega_n} \tag{26}$$

And the phase angle, ϕ, can be calculated using:

$$\phi = -\ acot(\frac{c\omega}{k - \omega^2 m}) \tag{27}$$

("Forced Oscillations")

Piezoelectricity

There are multiple ways to harvest electrical power, including piezoelectricity, rotational electromagnetism, linear electromagnetism, and triboelectricity. The piezoelectric effect is the ability of certain materials to generate an electric charge in response to applied mechanical stress. One characteristic of the piezoelectric effect is that it is reversible. Materials exhibiting the direct piezoelectric effect also show the converse piezoelectric effect, which is the generation of stress when an electric field is applied. Another interesting part of the piezoelectric effect is that a shifting of the positive and negative charge centers in the material takes place, which then results in an external electrical field. When reversed, an outer electrical field either stretches or compresses the piezoelectric material. Piezoelectric systems are useful when trying to generate high voltages and with electronic frequency generation. Some examples of naturally occurring piezoelectric materials are Berlinte, cane sugar, quartz, topaz, Rochelle salt, and bone. There are also man-made piezoelectric materials, such as barium titanate and lead zirconate titanate ("The Piezoelectric Effect").

When it comes to piezoelectric generators, two materials have led the way, macro fiber composite (MFC) and lead-zirconate-titanate (PZT). Out of those two, MFC transducers have lower energy density and power generation but are designed to be extremely flexible and highly resistant to damages. PZT is more effective in a random vibration environment. However, raw PZT material is brittle and has a resonant frequency higher than what is commonly found in industrial applications. This makes it difficult to implement for custom harvesters (Cryns et al.). A quick pack (QP) actuator can be used as a transducer. A QP actuator is a bimorph piezoelectric device that uses monolithic piezoceramic material mixed with an epoxy medium. Since QP uses monolithic piezoceramic material, it is more rigid than MFC, and is more resistant to damage than raw monolithic piezoceramic material (Shan, Song, Liu, Xie).

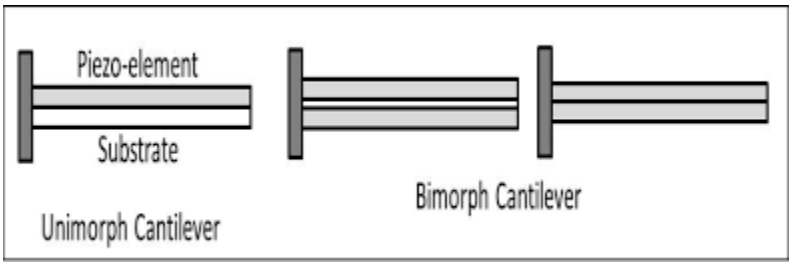

Figure 4: Depiction of Basic Cantilevers (Kumari, Khanna 2)

There are two different kinds of cantilevers to look into. There is a bimorph cantilever, which is used for actuation or sensing which consists of two active layers. The active layers are the piezoelectric elements. It has a passive layer between the two active

layers called the substrate. In contrast, a piezoelectric unimorph has only one active (piezoelectric) layer and one passive (substrate) layer. For a unimorph cantilever, the active layer will expand and the passive layer will contract if voltage is applied, thus the unimorph bends. In sensing applications, bending the unimorph produces voltage which can be used to measure displacement or acceleration. This mode can also be used for energy harvesting (Kumari, Khanna 2).

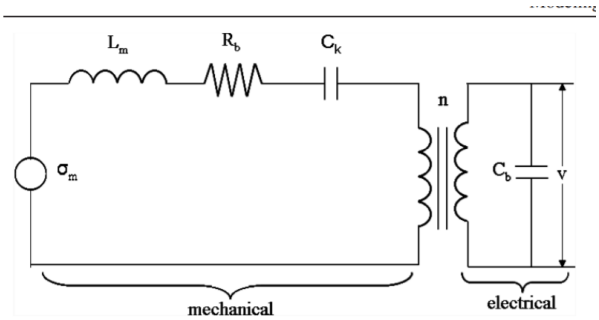

Figure 5: Circuit Representation of a PZT Beam

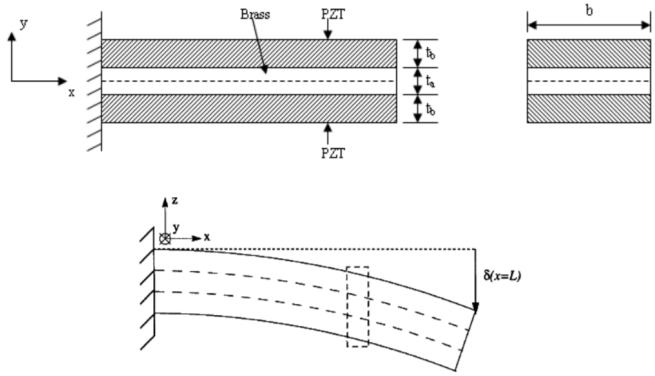

Figure 6: Geometry of the Beam (Ajitsaria et al 448-449)

The picture above shows a basic geometry of the bimorph cantilever. Brass is used in this particular example as a substrate, but other substrates can be used, such as stainless steel or copper. Pure elasticity is located between the upper and lower layers of the PZT material. The design of this structure neglects shear effects and ignores residual stress-induced curvature. Also, the radius of curvature for all the layers is assumed to be close to the same compared to those of the structure, simply because of the assumption that the thickness is much less than the overall beam curvature (Ajitsaria et al 448-449).

Electrical power *P* of a piezo transducer can be calculated from the bending normal strain of the piezo composite cantilever using:

$$P = \gamma^2 E^2 K_{33} \varepsilon_0 g_{31}{}^2 LWTf \quad (28)$$

Where γ is the normal bending strain at the furthest point of the piezo to the neutral axis, E is the elastic modulus of the composite, K_{33} is the Relative Dielectric Constant of the piezo material, ε_0 is the universal constant of vacuum permittivity, g_{31} is the piezoelectric constant of the piezo material representing the ratio of the strain (in direction 1) produced to the charge density (in direction 3) (Carter & Kensley). Figure 7 shows the different directions referenced by the numbers in the subscripts of K_{33} and g_{31} along with their respective axes (American Piezo). L, W, and T are the length, width, and thickness of the cantilever, respectively. f is the oscillating frequency of the cantilever.

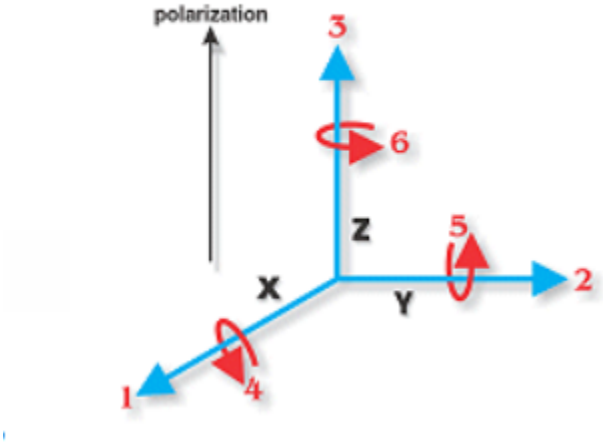

Figure 7: Directions of Forces Affecting a Piezoelectric Element (American Piezo)

Piezoelectric Energy Harvesting from Fluid Flow Example

In the background of their experiment, Taha Çıkım, Devrim Gözüaçık, and Ali Koşar describe similar experiments to their own. One experiment they examined was an experiment with a piezoelectric harvesting device. This device harvested energy from flow induced vibrations using piezoelectric films. For a vibration frequency of 26 Hz, the max output power of this device was 0.2 μW, with an output voltage of 2.2 V (1318).

In their own experiment, Çıkım et al. designed a device to include durability, a waterproof body, longevity, and ability for the device to adapt to different conditions. Their device used an aluminum case to protect the electrical components from humidity and water. Aluminum has a low density, helping keep the device light-weight, while also being resistant to corrosion. The device was small and light, which allowed it to be placed in areas that are difficult to reach. They used mini generators in their experiment, rather than piezoceramic materials (1320-1321).

The device was tested in a few different water salinities. In the simulation, fresh water was tested, with a theoretical maximum power of 6.45 W at a fluid velocity of 5 m/s. Experimentally, the device only had a max power of 4.3 W in fresh water when the fluid velocity was 5 m/s. The minimum power found in the experiments was with high salinity water, where the salt concentration was about 350 g of salt in 1000 mL water. The minimum power found here was 1.54 W when the fluid velocity was 1 m/s (Çıkım et al 1326-1327).

The Design

A cantilever design was chosen because the team wanted to limit the number of moving parts within the system. In selecting a cantilever system, a piezoelectric generator was the most logical choice, as it matches the cantilever system better than electromagnetic generation.

The bluff body selected to create the VIV the system is harvesting energy from was selected mainly due to how well researched fluid flows over cylinders have been in the past. Once a bluff body becomes asymmetric, its orientation with respect to the flow plays a major role in the response of the system. Asymmetrical bluff bodies can undergo VIV but also galloping, which is a type of fluid induced vibration (FIV) with a large amplitude and a low frequency, compared to the shedding frequency (Seyed-aghazadeh et al. 1). We decided our bluff body will be a cylinder due to its symmetry to focus on VIV rather than galloping.

The main goal was to maximize the frequency to generate more power, which according to Equation 2 means a small diameter. However, a smaller diameter leads to a smaller lifting force according to Equation 3 as well as manufacturing and assembly difficulties. We then had to design a cantilever system that could interface with the cylinder and oscillate at the same frequency as the VIV from the water on the cylinder mass.

A basic design of a cantilever with a cylindrical mass attached at the end was initially created. This design of the cantilever used dimensions from the product S129-H5FR-1803YB at this link from Piezo.com. The figure below shows the original design.

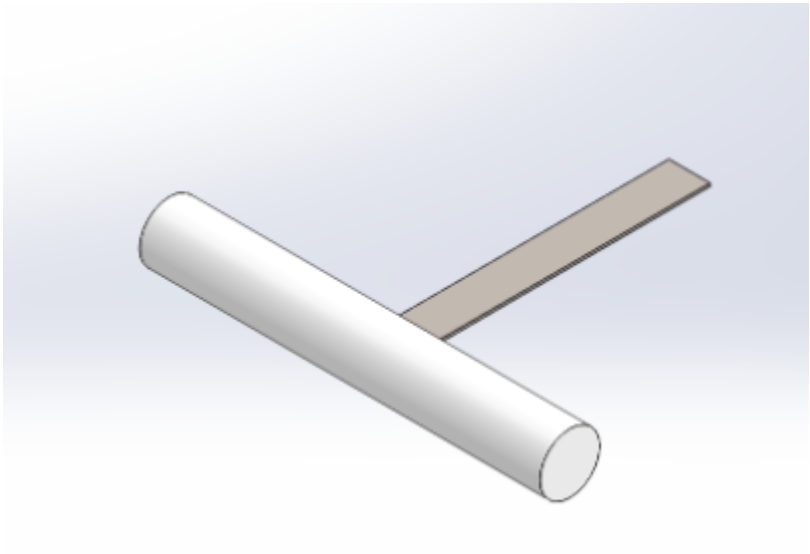

Figure 8: Isometric View of Initial Basic Design

This design was very basic and it did not account for how the cylinder would mount to the cantilever, how the cantilever would attach to a frame, nor how to equalize the shedding frequency of the VIV on the cylinder and the natural frequency of the cantilever.

The new system the team designed consists of two cantilever beams with a cylinder oriented horizontally at their ends. This cantilever beam is connected to an 80/20 frame, with a piezoelectric ceramic connected to the end of each beam opposite the cylinder. This piezoelectric ceramic will be connected to a harvesting circuit, which will be held out of the water by the frame. Images of the mechanical design can be seen below. The material of the cylinder was chosen to be ABS because of its ability to be 3D printed in detailed geometries along with its degradation resistance to water. The material of the cantilever is 6061 aluminum because of its high elastic modulus and its ease of being cut by a water jet. The choice of the cantilevers placed on the outside of the cylinder was designed with the intent to keep the fluid flow through the cylinder unblocked. The frame was chosen to be 30 mm 80/20 aluminum extrusion because of its ease of assembly. The updated design of the assembly can be seen in Figure 9 and Figure 10.

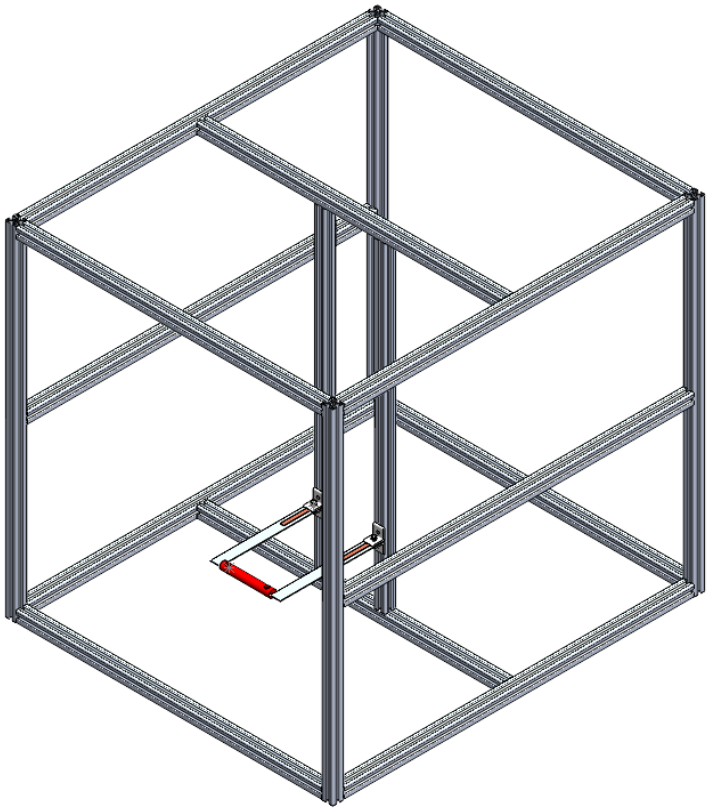

Figure 9: Isometric View of Harvester in Frame

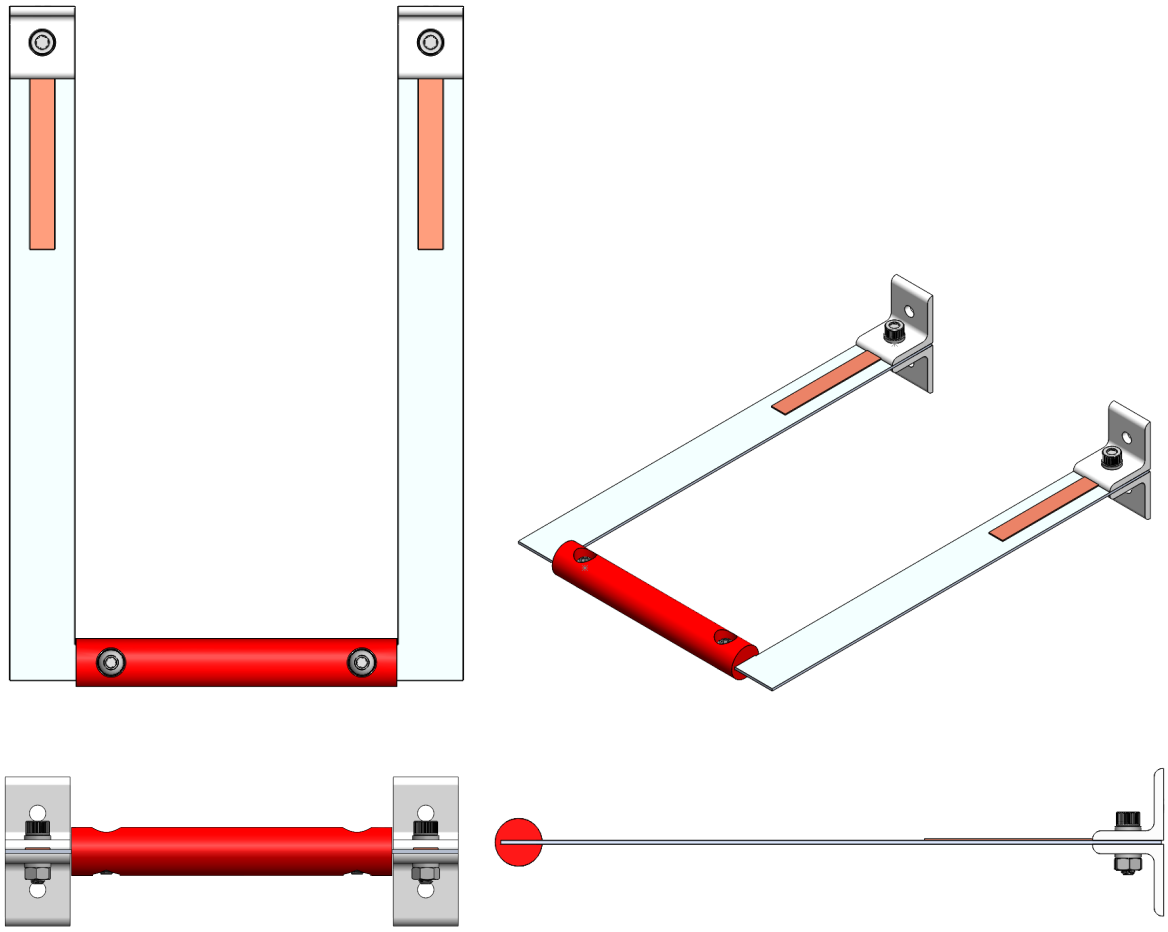

Figure 10: Isometric, Top, Front, and Right View of Harvester without Frame

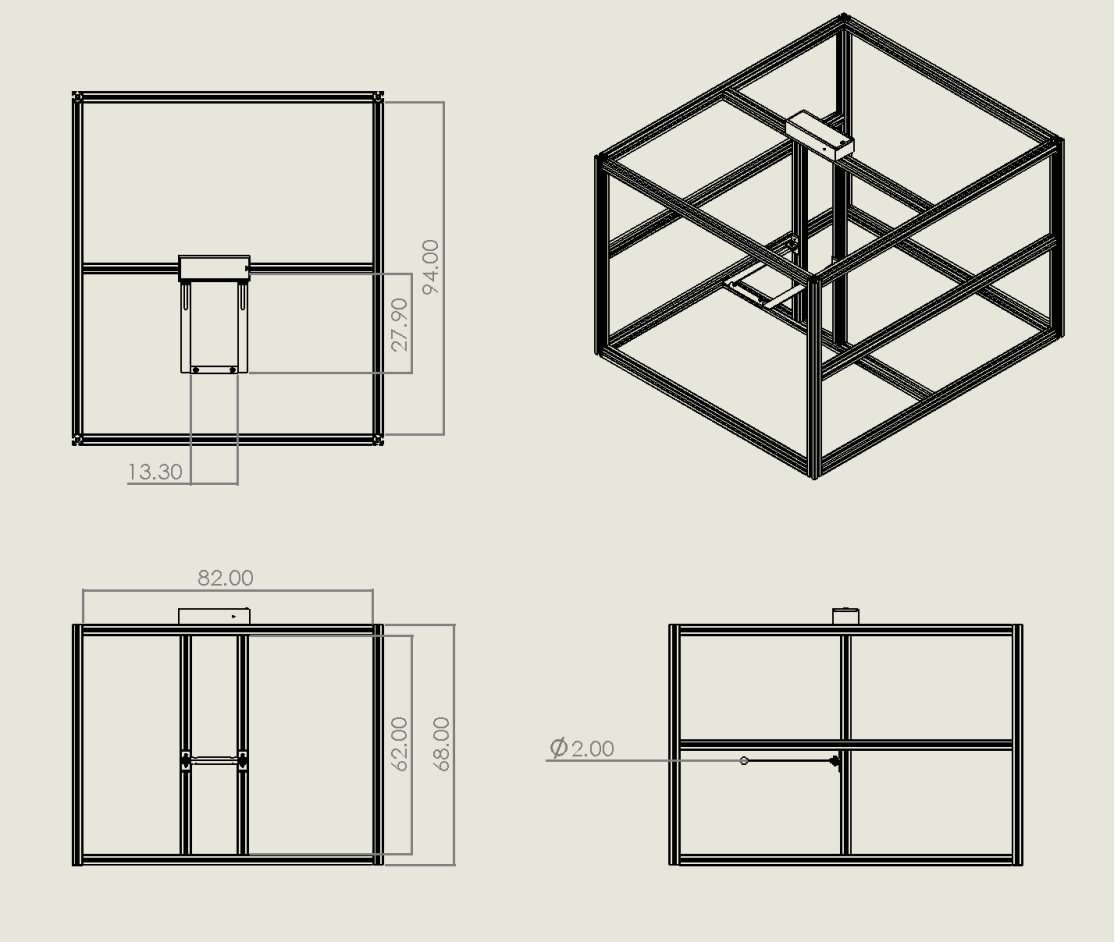

Figure 11: Dimensions in millimeters of Frame, Cantilever and Cylinder

Important factors included in design choices:

- Matching the excitation frequencies of the vortices on the cylinder with the natural frequency of the cantilever
- Keeping an open channel of water for the vortices after leaving the cylinder
- Achieving near neutral buoyancy of the cylinder mass in the water

Values for the water and cylinder can be seen in Table 1:

Table 1: Cylinder/Water Properties

Cylinder/Water Properties	Value	Units
Cylinder Diameter	0.020	m
Cylinder Length	0.134	m
Cylinder Volume	4.21E-05	m^3
Cylinder Density	1040	kg/m^3
Water Density	998	kg/m^3
Water Kinematic Viscosity	1.41E-06	m^2/s
Flow Speed	0.8	m/s
Reynolds Number	1.14E+04	N/N
Strouhal Number	0.200	Hz/Hz
Vortex Shedding Frequency	8.00	Hz
Mass of Displaced Fluid	0.0420	kg
Mass of Cylinder	0.0281	kg
Mass of Extra Piece of Beam and Nuts/Bolts	0.0174	kg
Mass Ratio	1.08	kg/kg
Lift Coefficient	0.500	
Lift Force	0.428	N

One value to note in the table above is the mass ratio being slightly above 1, meaning that the cylinder is near neutral buoyancy.

Values for the aluminum cantilever can be seen in Table 2:

Table 2: Aluminum Cantilever Properties

Aluminum Cantilever Properties	Value	Units
Young's Modulus	6.89E+10	Pa
Length	0.250	m
Base	0.0540	m
Height	0.00160	m
Area Moment of Inertia	1.84E-11	m^4
Density	2720	kg/m^3
Mass	0.0588	kg
Beam Natural Frequency	8.24	Hz
*f**	0.970	
Distance of Bottom of Strip to Piezo	6.40E-04	m
Dynamic Deflection at Resonance	0.0109	m
Equivalent Static Force	2.66	N
Stress	2.88E+07	Pa
Yield Strength	2.41E+08	Pa
Stress Safety Factor	8.36	
Strain at Piezo	3.76E-04	m/m
Max Allowable Strain	5.00E-04	m/m

Strain Safety Factor	1.33	

A few values are of interest in the table above. f^* is near 1, meaning that the system will reach resonance when the water nears 0.8 m/s. The strain is at a point where the piezo strip will not be damaged, but the goal is to increase that safety factor as it is near 1. The bending stress at the fixed point of the cantilever is currently well below the yield strength for a safety factor of over 8, meaning that even if the mass-cantilever system achieves resonance, the aluminum should not yield. The cantilever base value of 0.054 m is the two cantilever widths combined for dynamic deflection and spring constant calculations.

In developing the circuit to harvest the energy generated by the piezoelectric strips, the first thing to determine was how the energy was generated. When the piezoelectric strips were received, one was connected to a digital multimeter, and the voltage was measured when bending the strip back and forth. This led to the generalization that the piezoelectric strips could be modeled as an alternating current (AC) source. To have a direct current (DC) output, we had to design a rectifying circuit. Our circuit uses a full wave bridge rectifier, consisting of four 1N4004 diodes. A filter capacitor was added after the diodes, connecting the positive and negative ends of the output, to limit the ripple in the output voltage. A 100μF was selected for this task, having been compared with a 330μF capacitor and a 50μF capacitor. Of these choices, the 100μF capacitor was chosen to balance the limiting of the ripple voltage and the current flowing through the circuit. The higher capacitance led to a lower voltage ripple, but the current flowing increased tremendously. The diodes can only handle a current up to about 1A. The 330μF capacitor allowed a current over 10A to flow, which in turn would have burned out the diodes. Using the 100μF capacitor limited the current to less than the single amp allowed. After the filter capacitor, a voltage regulator was placed to bring the rippling voltage to a nearly steady output voltage. An LM7805 voltage regulator was used. In the simulation, a 100kΩ resistor was used as a load. This allowed an expected voltage to be measured. The circuit was simulated using Multisim 14, and it is pictured in Figure 12.

As the system uses two piezoelectric strips, on either end of the oscillating cylinder, the team designed the circuit to rectify the voltage coming from each strip separately. This allows for the voltages coming from each piezostrip to add together, whereas having them added together without rectification could lead to the voltages canceling one another out, should they be moving out of phase with one another. Each strip is connected to a diode bridge and its own capacitor, and the positive side of one of the piezostrips after the capacitor connects to the negative of the other piezostrip after the capacitor. This allows for a higher output voltage.

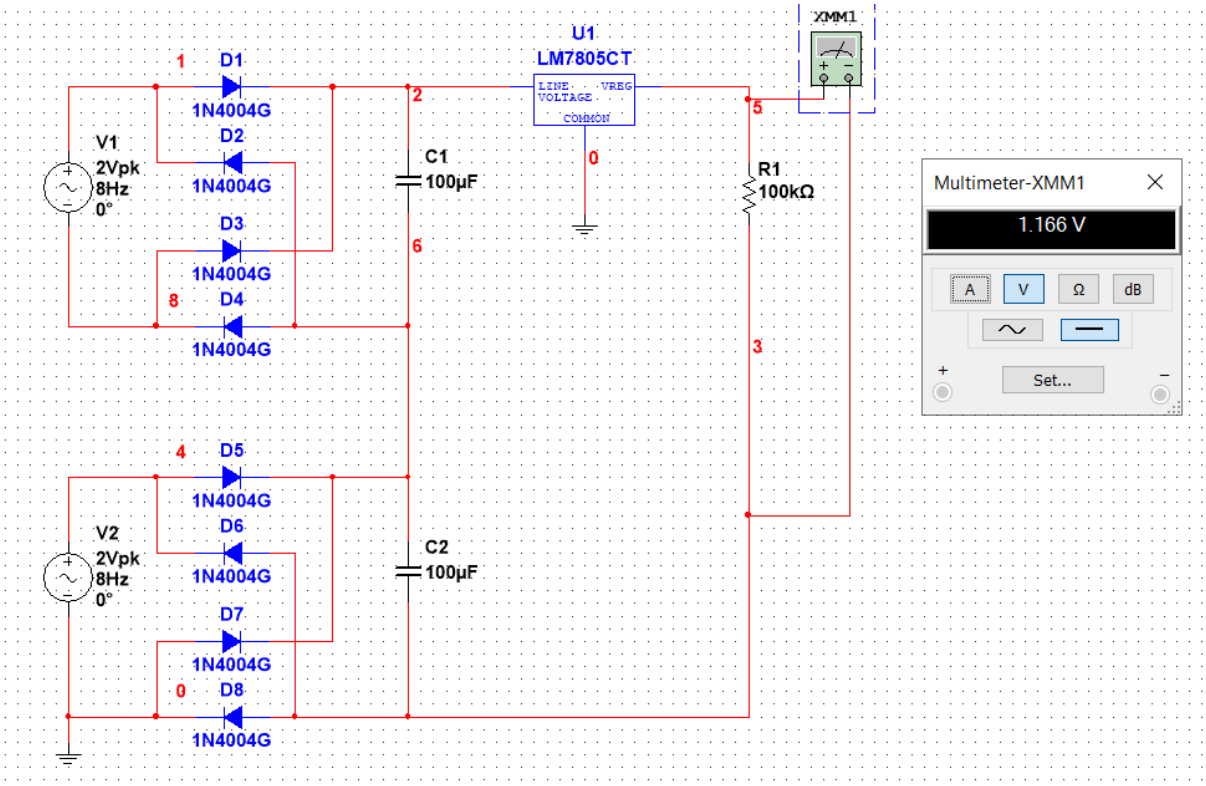

Figure 12: Simulated Circuit Diagram

Building Process

The 80/20 aluminum extrusions were initially cut down to size using a band saw. Since the band saw is not a very precise machine, a 2-3 mm buffer was left on the ends of the 80/20. To get a more precise cut, the extrusions were then taken to a Haas CNC Mill where the extrusions were milled down to size. The extrusions were assembled using 90 degree brackets. Figure 13 shows the assembled frame.

Figure 13: Assembled Frame

The aluminum cantilever was cut using a waterjet. The waterjet was chosen due to its accuracy compared to other cutting methods that were available to us. The piezoelectric transducers were adhered to the cantilevers using Loctite E-120hp Epoxy Adhesive. The cantilevers were rigidly clamped to the frame using corner brackets. The 3D printed cylinder was printed with two slots, one on each end of the cylinder. The cantilevers fit into these slots and were secured using nuts, bolts, and washers. Figure 14 shows the assembled cylinder-cantilever assembly.

Figure 14: Cylinder-Cantilever Assembly

In assembling the circuit, a breadboard was used for the base to allow for components to be easily switched if needed. Two sets of four diodes were arranged into diode bridges, one on either side of the breadboard. The end of each diode bridge was connected to a capacitor to filter the ripple in the output. These capacitors connected such that the voltages were connected in series together. The voltage regulator was connected to the positive side of one capacitor, which was then connected to the resistor load. The other end of the resistor load was connected to the negative end of the other capacitor.

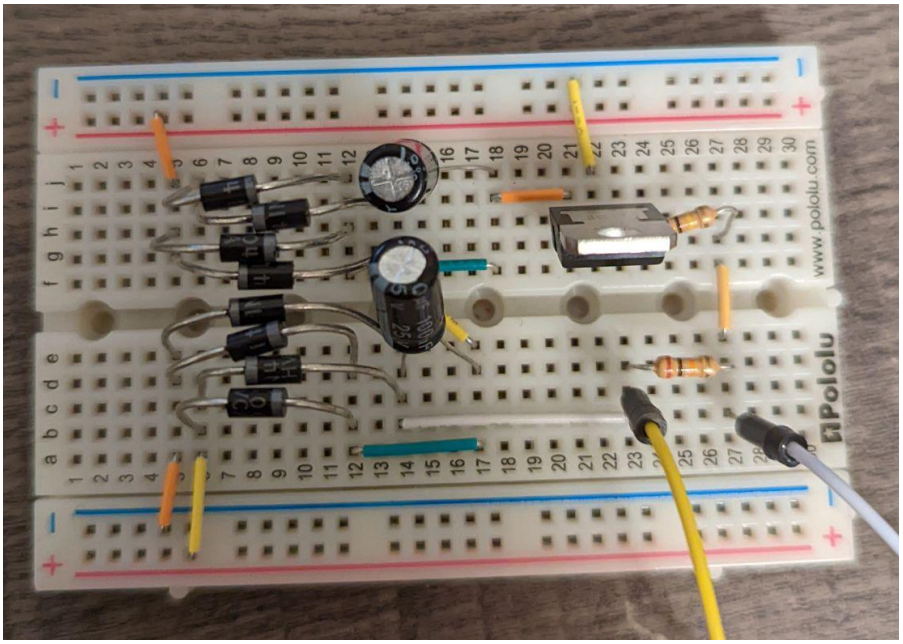

Figure 15: Assembled Circuit without the Connection to the Piezoelectric Strips

Once the electronics were assembled, the circuit and Arduino were put into a 3D printed case that would lay on top of the frame. Figure 16 shows the assembled Arduino-circuit case.

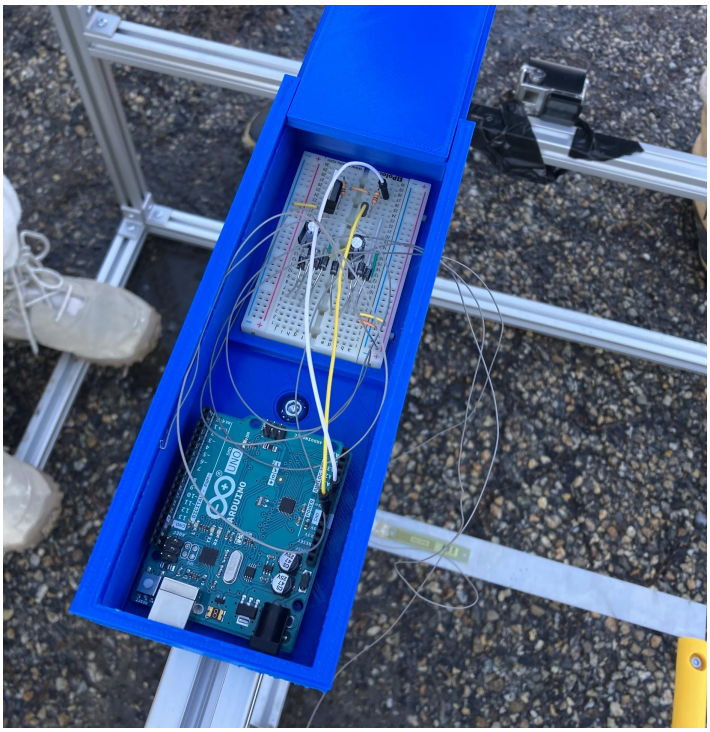

Figure 16: Arduino-Circuit Case Assembly

Finally, all the components were assembled and were ready for testing. Figure 17 and Figure 18 show the fully assembled device.

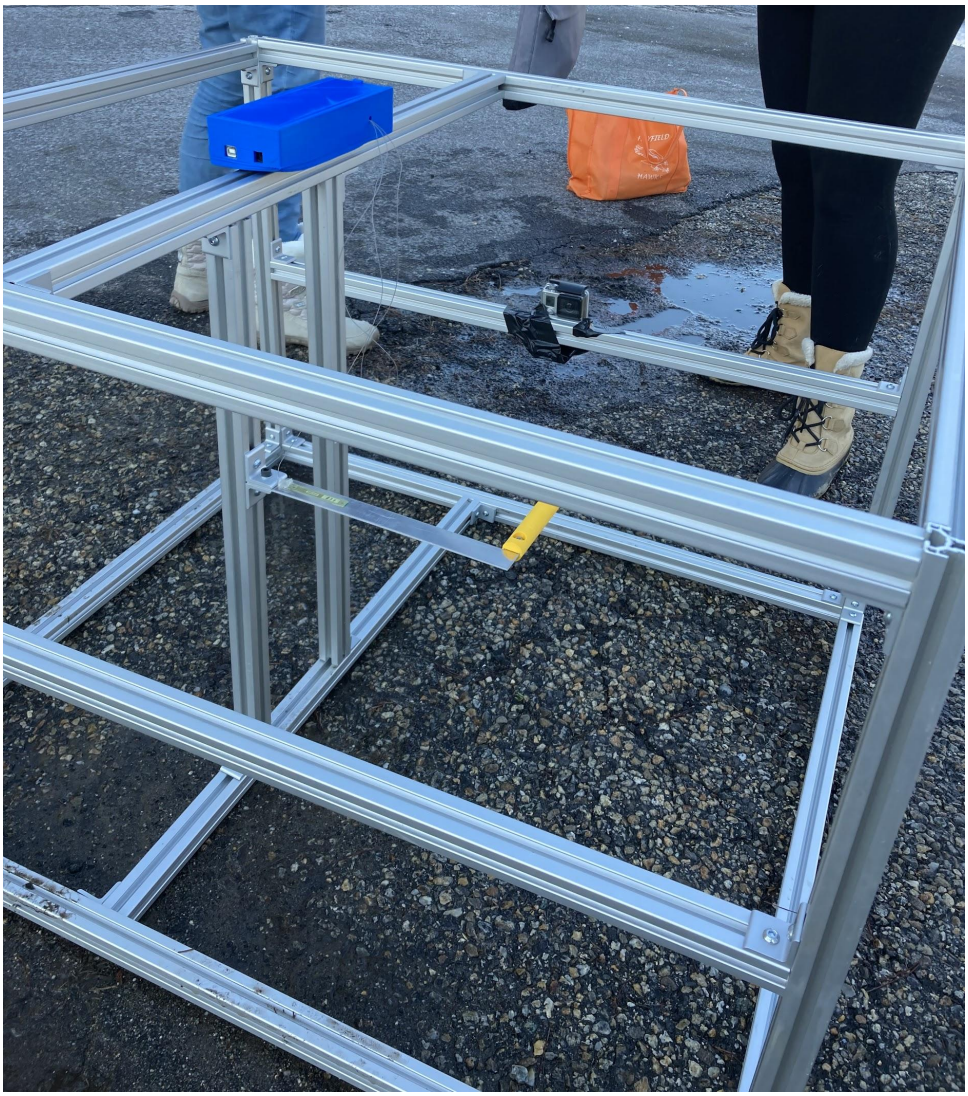

Figure 17: Fully Assembled Device

Figure 18: Side View of Fully Assembled Device

Testing and Data

When the time came to test our device, the first step was to locate a suitable place to conduct our experiments. Since our main goal was to harvest energy from flowing fluid, it was decided to find a river that meets our needs. The start of the French River located in Leicester, MA was selected as our testing site.

Piezoelectric Strips in Air

The first test was with just the piezoelectric strips in air. This test was to measure the natural frequency and damping coefficient of the piezoelectric strips, which was done by using an oscilloscope. One end of the strip was clamped and the free end was plucked. We measured the fluctuating voltage and calculated the damping of the piezoelectric transducer using the voltages at two consecutive peaks.

Table 3: Piezoelectric Strip in Air

Amplitude of Peak 1	44 V
Amplitude of Peak 2	29.6 V
Logarithmic Decrement	0.396
Damping of Piezo Strip ζ	0.0630
Damping Coefficient C	0.629 Ns/m

Cantilever in Air

The second test was conducted after the piezoelectric strips were adhered to the cantilever. The cylinder was also attached to the cantilever and this test was also conducted in air. The ends of the cantilever were clamped and the cylinder was plucked. This test was conducted multiple times and we were able to calculate the damping coefficient using 4 peaks the first time and 5 peaks the second time. The natural frequency of the system in air was also recorded.

Table 4: Cantilever in Air

Cantilever	Test 1	Test 2
Amplitude of Peak 1	8.4 V	13.8 V
Amplitude of Peak 2	8 V	13.4 V
Amplitude of Peak 3	7.84 V	13 V
Amplitude of Peak 4	7.6 V	12.7 V
Amplitude of Peak 5	N/A	12.4 V
Logarithmic Decrement δ	0.0250	0.0214
Damping of Cantilever ζ	0.00398	0.00341
Damping Coefficient C	0.0396 Ns/m	0.0339 Ns/m

Cantilever in Static Water

The third test was conducted in a static bucket of water which gave us the damping of the system when submerged in water. We once again used an oscilloscope to measure the voltage peaks and calculated the damping while submerged in water using 3 peaks.

Table 5: Cantilever in Static Water

Cantilever in Water	
Amplitude of Peak 1	11 V
Amplitude of Peak 2	4.6 V
Amplitude of Peak 3	2.6 V
Logarithmic Decrement δ	0.481
Damping of Cantilever ζ	0.076

Damping Coefficient C	0.759 Ns/m

Fully Assembled Frame in River

With all the preliminary testing done, the group brought the fully constructed frame and cantilever to the French River. Before each test, the conditions of the river were noted which included the velocity, depth, and temperature of the water. The frame was then submerged in the river.

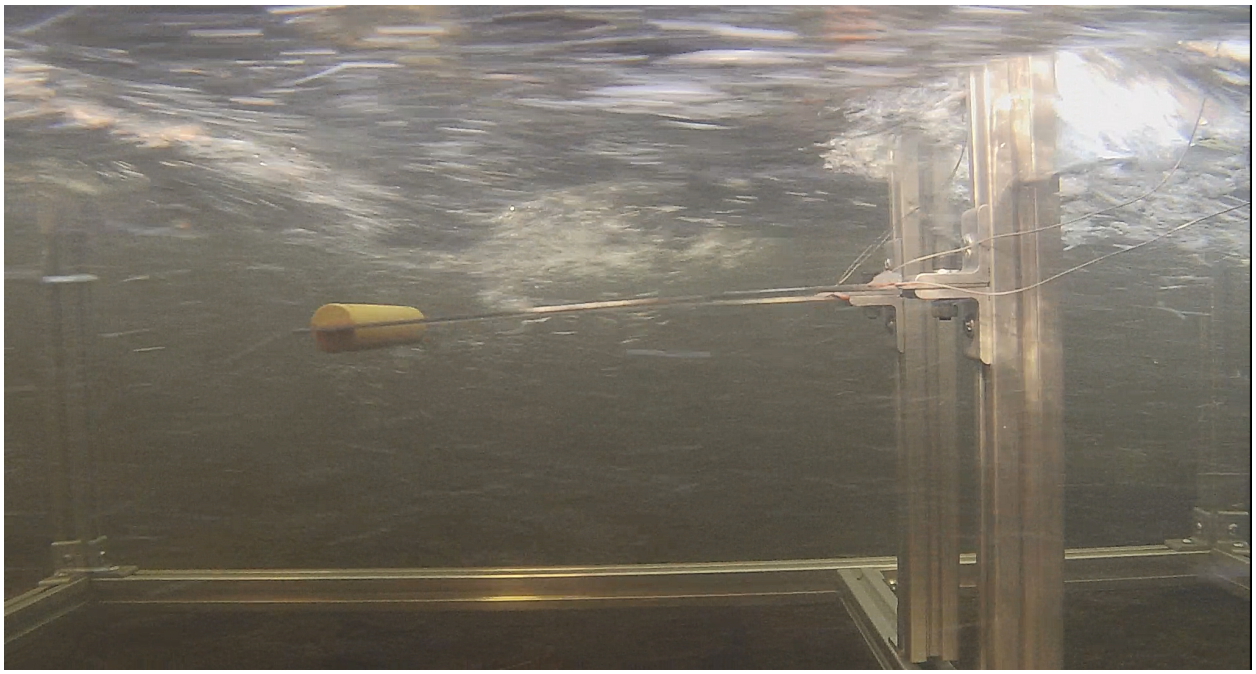

Figure 19: Cantilever Submerged in River

Once in the water, we measured the circuit's output voltage using the Arduino Uno. The output voltage was measured by connecting the Arduino over the resistive load. The measured voltage output was recorded in the Arduino app then moved to an Excel sheet. In this sheet, the average of the measured outputs were taken. Since the AC voltages are being rectified, the output voltage was more DC. This meant getting a shedding frequency from the Arduino was not possible to do. Instead, video was taken under the water using a GoPro Camera. The position of the cantilever was tracked and we calculated a frequency using the total peaks over the time. Due to a technical error, we were unable to record the cantilever on March 8th. This led to us not being able to get an observed frequency or max deflection.

Table 6: Data Collected from Tests in the French River

Date	Air Temp (°C)	Water Temp (°C)	Average Velo (m/s)	Highest Velo (m/s)	Calc Freq (Hz)	Observed Freq (Hz)	Observed Max Deflection (m)	Average Voltage (V)	Depth (in)	Calc Power over Resistance (μW)
2/17	13.89	1.6	0.6	1	6	5.6	0.00680	0.08	14.5	0.05
2/21	12.78	2	0.5	0.9	5	5.9	0.0140	0.45	15	1.68
2/23	13.89	3.5	0.9	1.3	9	6.4	0.0137	0.54	16	2.92
3/2	3.89	1.6	0.7	1.3	7	6.6	0.00853	0.48	17.5	2.30
3/8	5.56	3.8	0.9	1.6	9	N/A	N/A	0.56	14	3.14

The first test on February 17th used only one piezoceramic strip, as the leads to the second one disconnected prior to the test. By the second test on February 21st, we had both piezoceramic strips fully connected to our circuit. When the voltage output measured was well over double the voltage from the first test, we realized something must be wrong with one of our two piezoelectric strips. To find this error, the two piezoelectric strips were tested separately as well as together during the testing on February 23rd.

Figure 20: Top View of Cantilever with Piezoelectric Strips Labeled

Table 7: Average Voltages of Each Piezoelectric Strip During Test on 2/23

Piezoelectric Strip	Average Voltage (V)
A	0.07
B	0.32

In testing the strips separately, we found one piezoelectric strip gave a voltage of over four times the output of the other. As we had used one of the piezoelectric strips in our preliminary testing for the damping coefficients, we thought we may have accidentally overstressed that strip, and we replaced it on our cantilever for our final two tests. The other piezoelectric strip was also replaced just before the last test.

Data Analysis

Deflection

From Table 2, the calculated dynamic deflection is 1.09 cm. The max deflection while the cantilever was in the river was found by using the Gopro video and the Tracker app. These deflections can be seen in Table 6. On February 22nd and 23rd, the max deflection was 1.40 cm and 1.37 cm respectively, both of which is greater than the calculated dynamic deflection. On March 2nd, the max deflection was 0.853 m and February 17th was 0.680 cm.

Voltage and Power

When doing our preliminary calculations, we assumed the flow velocity to be 0.8 m/s. As seen in Table 6, the real world conditions of the river never aligned with what we had assumed. There were three test days in which the power was over two microwatts, February 23rd, March 2nd and 8th. All of these days had relatively close flow velocities to the assumed 0.8 m/s. This can be attributed to the fact that we designed the cylinder to have a vortex shedding frequency of 8 Hz and the system to have a natural frequency of 8.24 Hz. February 17th and 21st had average flow speeds of 0.6 m/s and 0.5 m/s, respectively, which is quite lower than the assumed 0.8 m/s. This resulted in a lower calculated vortex shedding frequency and a lower observed frequency, which eventually led to a lower power output. Out of the three days above two microwatts, March 8th had the greatest voltage and power output. This is likely due to the fact that both piezoelectric strips were changed and were not overstressed prior to testing and the average velocity was within 0.1 m/s of the assumed 0.8 m/s.

Power Ratio and Efficiency

Our major inspiration for this project was the VIVACE device, which used a rotary electrical generator rather than piezoelectric strips. This device had a power ratio of $\eta_{VIVACE} = 0.22$ achieved experimentally for U=0.84 m/s. The upper limit of VIVACE power ratio was $\eta_{UL-VIVACE} = 0.37$ (Bernitas et. al).

The power ratio is calculated using:

$$\eta = \frac{P_{VIVACE-harnessed}}{P_{fluid}} \tag{29}$$

For our device, the maximum power harvested was 3.14 μW, measured on March 8th. The corresponding fluid power calculated from the same measured values is 1.083 W. From this, our system's power ratio is $\eta_{sys} = \frac{P_{sys-harnesses}}{P_{fluid}} = \frac{3.14*10^{-6}}{1.083} = 2.9 * 10^{-6}$.

We were also able to find potential energy stored in the cantilever using:

$$PE = \frac{1}{2}kx^2 \tag{30}$$

The potential energy stored based on a max deflection of x = 0.0140 m is $2.39 \times 10^{-2} J$.

The mechanical power, P_{mech}, exerted by a cantilever can be calculated using:

$$P_{mech} = PE * f \tag{31}$$

When our system achieved this max deflection, the mechanical power of the cantilever equaled 0.153 W. The fluid power from this day was 0.334 W. This gives our mechanical efficiency to be about 46%.

Conclusion

While we got a measurable voltage output from our system, we did not get a high enough power at any point to readily power something like a small LED light. Therefore, over the course of our project, we only took measurements.

We observed minimal twisting in our system, meaning the two cantilevers were mostly in phase with each other. So we believe that we did not need our circuit to rectify the voltages separately. We could have changed the circuit to connect the piezoelectric strips' leads in series prior to being rectified. As each of the 1N4004 diodes has approximately a 1 V voltage drop over it, we could have greatly increased the voltage output of our system by rectifying the input together. Theoretically and looking at circuit simulations done prior to the assembly of the system, the output voltage could have increased by 1-1.5 V by rectifying the piezoelectric strips together.

The max deflections were seen both above and below the calculated dynamic deflection. This could be from a number of different reasons. Some possibilities include the variation in vortices due to the inconsistent flow, potential lower damping constant in flowing water, and possibly a higher lift coefficient. To confirm these possibilities, more testing would need to be done in the future. The lift coefficient could be found experimentally rather than assumed and the damping constant could be found in flowing water rather than just static.

At the conclusion of our project, we wanted to think of some ways we could change or alter our project to be able to get better results. One way we thought to make our project better was to add more piezoelectric strips to the prototype that we used for our project. We would add two more strips to the underside of the cantilever. The thought behind this was that we could gain more power from the different bending motions that the cantilever will undergo in the flowing water, since the water flow is never truly constant. Therefore, we can get more power no matter how the cantilever bends.

In reality, though, the piezoelectric strips do not lend themselves well to scaling. They are best used for smaller sensors or projects that require smaller amounts of power to run. They do work well in water, so using it to power a sensor for something like a change in speed or change in height of flowing water would be an ideal service for these smaller energy harvesters. There are other sensors that could be in the range for the piezoelectric harvesters that do not need to be in water. Some examples are an image sensor and a gas sensor. An image sensor can use a piezoelectric plate to determine the characteristics of a resonance or antiresonance vibration performance in something like a camera. Gaseous piezoelectric sensors are found in medicine, agriculture, and other environmental monitors. They are relatively simple in preparation and application, and are inexpensive. These devices allow for the identification and determination of substances in their gaseous and liquid phases.

In a redesign, we also would do further analysis on the cyclic loading from the lift force on the cantilever. Aluminum, being a material without any fatigue limit, may present issues once the system reaches many cycles. A material like steel may be more suitable if we make sure that the stresses stay below steel's fatigue limit. This would result in the cantilever theoretically being able to oscillate infinitely in a current of water without failing. In this redesign, due to a higher spring constant/elastic modulus of the material, geometries of the cantilever would need to be changed so that the natural frequency of the cantilever system is close to the vortex shedding frequency. We would also look into using a different type of generator that would be able to convert more of the mechanical energy to usable electrical energy.

Broader Impacts

The code of ethics for engineers states that an engineer will put the safety of others and the enhancement of human welfare at the forefront of their work. In this practice, the team has worked to create a sustainable source of harvesting energy. This will allow for a healthier environment and atmosphere, which will in turn improve the health of the people. Another fundamental portion of engineering ethics is that an engineer will work only in areas of their own competence. This was followed by the team devising different portions of designing and building this system. Some worked to 3D print, or machine the metal for the frame and the cantilever. Others worked to assemble the pieces or to design and build the circuit to provide usable electrical energy.

The environmental impact of the system detailed in this report was designed to be minimal. The original VIVACE device is theorized not to have any impact on fish or other marine life. This is due to the fact that a system designed to utilize the VIV is similar to how a fish moves. When a fish swims through water, it forms little vortices behind itself, which, when shed, moves the fish forward (Bernitsas et al). This similarity in the motions of the water around both the fish and the system means that fish will not be affected by a machine using VIV. Additionally, as the device is expected to move slowly, our design at only 8Hz, gives plenty of time for a marine creature to move around the oscillating cylinder. This also allows for minimal impact on the environment where the system is implemented.

Works Cited

Bernitas, M. M., Raghavan, K., Ben-Simon, Y., and Garcia, E. M. H. (September 16, 2008). "VIVACE (Vortex Induced Vibration Aquatic Clean Energy): A New Concept in Generation of Clean and Renewable Energy From Fluid Flow." ASME. J. *Offshore Mech. Arct. Eng.* November 2008; 130(4): 041101. https://doi.org/10.1115/1.2957913

Blevins, Robert D. *Flow-induced Vibration*. 2nd ed., New York City, Van Nostrand Reinhold, 1990.

Carter, R. & Kensley, R. *Introduction to Piezoelectric Transducers*. Piezo.com. https://piezo.com/pages/intro-to-piezoelectricity

Coburn, T., & Farhar, B. (2004). Public Reaction to Renewable Energy Sources and Systems. Encyclopedia Of Energy, 207-222. doi: 10.1016/b0-12-176480-x/00462-9

Cryns, Jackson W., et al. "Experimental Analysis of a Piezoelectric Energy Harvesting System for Harmonic, Random, and Sine on Random Vibration." *Advances in Acoustics and Vibration*, vol. 2013, 4 Aug. 2013, pp. 1-12, https://doi.org/10.1155/2013/241025.

Çıkım, Taha, et al. "Power Reclamation Efficiency of a Miniature Energy-Harvesting Device Using External Fluid Flows." *International Journal of Energy Research*, vol. 38, no. 10, 13 Jan. 2014, pp. 1318-30. *Wiley Online Library*, https://doi-org.ezpv7-web-p-u01.wpi.edu/10.1002/er.3149. Accessed 22 Sept. 2021.

Derksen, A. *Numerical Simulation of a Forced-and Freely-Vibrating Cylinder at Supercritical Reynolds Numbers*. MS thesis. www.researchgate.net/publication/333751600_Numerical_simulation_of_a_forced_a

nd_freely-vibrating_cylinder_at_supercritical_Reynolds_numbers. Accessed 28 Sept. 2021.

“Forced Oscillations.” *Dhote Bandhu Science College.* March 2020, https://www.dbscience.org/wp-content/uploads/2020/03/BSC-SEM-II-PAPER-I-UNIT-II-FORCED-OSCILLATOR.pdf. Accessed 18 Nov. 2021.

Gürgöze, M. "On the Representation of a Cantilevered Beam Carrying a Tip Mass by an Equivalent Spring–mass System." *Journal of Sound and Vibration*, vol. 282, nos. 1-2, Apr. 2005, pp. 538-42, https://doi.org/10.1016/j.jsv.2004.04.006.

Huston, Ronald, and Harold Josephs. *Practical Stress Analysis in Engineering Design*. 3rd ed., e-book ed., Boca Raton, 2008.

Lienhard, J. H., "Synopsis of lift, drag, and vortex frequency data for rigid circular cylinders," Washington State University College of Engineering Research Division Bulletin 300, pp. 1–32, 1966.

The Lift Equation. *NASA*, 13 May 2021, www.grc.nasa.gov/WWW/K-12/rocket/Images/lifteq.gif. Accessed 16 Oct. 2021.

"The Piezoelectric Effect." *Nanomotion*, Johnson Electric Company, www.nanomotion.com/nanomotion-technology/piezoelectric-effect/. Accessed 17 Oct. 2021.

"Piezoelectric Constants." *APC International, Ltd.*, American Piezo https://www.americanpiezo.com/knowledge-center/piezo-theory/piezoelectric-constants.html

Seyed-aghazadeh, B., et al. "Flow-induced Vibration of Inherently Nonlinear Structures with Applications in Energy Harvesting." *Physics of Fluids*, vol. 32, no. 7, 1 July 2020, p. 071701, https://doi.org/10.1063/5.0012247. Accessed 20 Sept. 2021.

Szepessy, S., and P.W. Bearman. "Aspect Ratio and End Plate Effects on Vortex Shedding from a Circular Cylinder." *Journal of Fluid Mechanics*, vol. 234, Jan. 1992, pp. 191-217, https://doi.org/10.1017/S0022112092000752.

Thomson, William T. Theory of Vibration with Applications. 4th ed., e-book ed., London, CRC Press, 1993.

Williamson, C. H. K., & Govardhan, R. (2004). VORTEX-INDUCED VIBRATIONS. *Annual Review of Fluid Mechanics*, 36, 413-455. https://doi.org/10.1146/annurev.fluid.36.050802.122128

Zahari, M., et al. "The Effects of Spring Stiffness on Vortex-Induced Vibration for Energy Generation." *IOP Conference Series: Materials Science and Engineering*, vol. 78, 2 Apr. 2015, p. 012041, https://doi.org/10.1088/1757-899x/78/1/012041.

101, C., & Facts, C. (2021). Top 10 Clean Energy Myths & Facts: The Truth About Alternative Energy. Retrieved 18 October 2021, from https://www.inspirecleanenergy.com/blog/clean-energy-101/3-clean-energy-myths